Real-Time, High-Resolution, Space–Time Analysis of Sea Surface Temperatures from Multiple Platforms

STEVEN M. LAZARUS, COREY G. CALVERT, AND MICHAEL E. SPLITT

Florida Institute of Technology, Melbourne, Florida

PABLO SANTOS

National Weather Service, Miami, Florida

DAVID W. SHARP, PETER F. BLOTTMAN, AND SCOTT M. SPRATT

National Weather Service, Melbourne, Florida

(Manuscript received 5 July 2006, in final form 1 December 2006)

ABSTRACT

A sea surface temperature (SST) analysis system designed to initialize short-term atmospheric model forecasts is evaluated for a month-long, relatively clear period in May 2004. System inputs include retrieved SSTs from the Geostationary Operational Environmental Satellite (GOES)-East and the Moderate Resolution Imaging Spectroradiometer (MODIS). The GOES SSTs are processed via a sequence of quality control and bias correction steps and are then composited. The MODIS SSTs are bias corrected and checked against the background field (GOES composites) prior to assimilation. Buoy data, withheld from the analyses, are used to bias correct the MODIS and GOES SSTs and to evaluate both the composites and analyses. The bias correction improves the identification of residual cloud-contaminated MODIS SSTs. The largest analysis system improvements are obtained from the adjustments associated with the creation of the GOES composites (i.e., a reduction in buoy/GOES composite rmse on the order of 0.3°–0.5°C). A total of 120 analyses (80 night and 40 day) are repeated for different experimental configurations designed to test the impact of the GOES composites, MODIS cloud mask, spatially varying background error covariance and decorrelation length scales, data reduction, and anisotropy. For the May 2004 period, the nighttime MODIS cloud mask is too conservative, at times removing good SST data and degrading the analyses. Nocturnal error variance estimates are approximately half that of the daytime and are relatively spatially homogeneous, indicating that the nighttime composites are, in general, superior. A 30-day climatological SST gradient is used to create anisotropic weights and a spatially varying length scale. The former improve the analyses in regions with significant SST gradients and sufficient data while the latter reduces the analysis rmse in regions where the innovations tend to be well correlated with distinct and persistent SST gradients (e.g., Loop Current). Data thinning reduces the rmse by expediting analysis convergence while simultaneously enhancing the computational efficiency of the analysis system. Based on these findings, an operational analysis configuration is proposed.

1. Introduction

Providing timely and accurate weather forecasts remains a priority of the National Oceanic and Atmospheric Administration (NOAA). These forecasts can be especially challenging within the Florida coastal zone (i.e., within 100 km of the coast), in the presence of sharp thermal gradients as evident along the land–sea interface, but also because of significant gradients in the nearshore sea surface temperatures (SSTs). Within the Florida coastal zone resides a considerable percentage of the state's population (with notable density) along with substantial marine-related interests both at the coast and just offshore. Efforts to improve environmental prediction through short-term weather forecasts will have a direct positive impact on area commerce and enhance opportunities for protecting life

Corresponding author address: Dr. Steven M. Lazarus, Florida Institute of Technology, 150 W. University Blvd., Melbourne, FL 32901.
E-mail: slazarus@fit.edu

DOI: 10.1175/MWR3465.1

during hazardous events (either natural or man induced). Importantly, gradients in SSTs can affect boundary layer evolution (e.g., Warner et al. 1990), seabreeze development, stratocumulus development (e.g., Young and Sikora 2003), offshore marine thunderstorms, coastal shower events, and so on. The ability, therefore, to include current mesoscale SST analyses within the forecast and analysis cycle is highly desirable. For example, recent work examining model output winds from the European Centre for Medium-Range Weather Forecasts (ECMWF) has shown that including higher-resolution SSTs has a positive feedback (and impact) on the surface wind stress field (Chelton and Wentz 2005; O'Neill et al. 2005; Chelton 2005). On the global scale, the desired SST accuracy is on the order of a maximum bias of 0.5°C at temporal scales of less than a day and resolution of at least 10 km (Smith 2001). For short-term high-resolution (less than 10-km resolution) mesoscale forecasts, required accuracies are on the order of 0.2°C (Donlon 2002). In a separate validation effort involving short-term high-resolution model forecasts, SST differences on the order of 1°–2°C over 100 km produce relatively significant differences (greater than 60 W m^{-2}) in the mean latent heat flux along the Florida Current (FC).

While SST satellite "snapshots" are fairly easy to obtain, they are not practical from the data assimilation and modeling perspective. Nonetheless, multiplatform derived SSTs are an excellent source of high-resolution data for operational analyses (He et al. 2004; Thiébaux et al. 2003; Reynolds and Smith 1994). In the absence of clouds and sun glint, infrared (IR) and near-infrared-based satellite sensors can consistently provide reliable radiances from which bulk (i.e., upper meter) SST estimates are derived. However, because operational analysis systems generally require contiguous (i.e., no missing data) gridded first-guess fields, some form of compositing is essential. Various compositing techniques may leverage either previous analyses or forecasts, or both. One common approach is a method whereby the warmest pixel or average of the warmest pixels (within a specified region and time window) is used (Haines et al. 2006; Walker et al. 2003; Glenn and Crowley 1997). This approach is designed to minimize cloud contamination but can be problematic during periods of seasonal or short-term variations in SST such as hurricane-induced upwelling. For our use, applications that are strictly designed to produce a gridded SST product by combining (e.g., averaging) observations over a given temporal window are herein referred to as compositing.

For the most part, current operational multiplatform SST analyses are global and run once per day, such as those systems at the National Centers for Environmental Prediction (NCEP)/Marine Modeling and Analysis Branch (MMAB) and the Met Office (UKMO). These global SST analysis systems were designed to initialize the suite of operational large-scale models running at the various weather centers and were not intended for use within high-resolution mesoscale models. The NCEP Real-Time Global Sea Surface Temperature analysis (RTG-SST; Thiébaux et al. 2003) has a horizontal resolution on the order of 0.5° (latitude, longitude). A 1/12° resolution SST product is also produced operationally by the MMAB; however, it is the RTG-SST that is used to initialize many of the North American and global models. At the time of this writing, the North American Mesoscale model, the Rapid Update Cycle model, and the ECMWF global model are all initialized using the RTG-SST. NCEP's Global Forecast System model uses the older Reynolds and Smith (1994) optimum interpolation analysis. The UKMO also generates, once per day, a separate high-resolution SST analysis (Lorenc et al. 1991) to initialize their mesoscale forecast model.

For real-time satellite data assimilation, primary issues include accuracy, resolution, and data latency. While a combination of both IR and microwave estimates of SSTs can help mitigate cloud impacts, SSTs derived from microwave estimates are of relatively coarse resolution (on the order of 25 km). Geostationary Operational Environmental Satellites (GOES) can provide SST data at temporal resolutions unattainable by polar orbiters and spatial resolutions on the order of 6 km. GOES SSTs have been shown to have errors less than 0.5°C, which are comparable to that of the higher-resolution Advanced Very High Resolution Radiometer (AVHRR; Walker et al. 2003). As part of a Cooperative Program for Operational Meteorology, Education, and Training (COMET) funded project, the Florida Institute of Technology has created a near–real time operational SST analysis system. This system is designed to provide high-resolution SST analyses, in lieu of the RTG-SST, to support mesoscale modeling initiatives over Florida and the adjacent coastal waters. In particular, the National Weather Service (NWS) in Melbourne, Florida, was cycling a version of the Advanced Regional Prediction System (ARPS; Xue et al. 2001) 4 times per day over an approximate 500-km^2 domain that includes all of Florida, the eastern Gulf of Mexico (GOM), the Florida Straits, and the northwest Bahamas (hereafter referred to as FL-ARPS). The analysis component, the ARPS Data Analysis System (ADAS; Brewster 1996), is run in near–real time and updated every 15 min over an 800-km^2 domain but does not analyze for SST. A parallel effort is also underway

to support a version of the Weather Research and Forecasting model under similar constraints. Here, a prototype SST analysis system has been configured to run over a region consistent with, but slightly smaller than, the operational (NWS) analysis domain (i.e., on the order of 700 km^2; Fig. 1). The analysis combines high-resolution SST data obtained from the imager on the *GOES-12* satellite and the Moderate Resolution Imaging Spectroradiometer (MODIS) onboard the *Aqua* and *Terra* satellites.

Relevant aspects relating to the development of the end-to-end operational analysis system are discussed here including 1) quality control (QC), 2) bias and trend corrections (BC and TC, respectively), 3) latency-related diurnal adjustment (DA), 4) spatially varying error covariances and decorrelation length scales, 5) data thinning, and 6) analysis isotropy. The impact of each of these is evaluated using a training dataset over which analyses are performed and then compared against buoy data. May 2004 is selected in part because regional cloud cover tends to be at a minimum while the coastal zone SST gradient along the western edge of the FC is pronounced (i.e., on the order of 3°–4°C).

2. Data

a. GOES-12

The GOES SST data are provided by NOAA/National Environmental Satellite, Data, and Information Service (NESDIS). The imager product, derived from the satellite radiances using 2 of the 5 available channels (3.9 and 11 μm), is a measure of the bulk SST, which is a representation of the temperature of the water column beneath the skin where turbulent heat transfer processes dominate (Donlon 2002). Thirty-minute data are combined to produce hourly SST files. The removal of both cloud-contaminated radiances and radiances that are affected by sun glint at 3.9 μm precede the application of a radiative transfer-based SST retrieval algorithm (Maturi et al. 2006). Man Computer Interactive Data Access System area files are subsampled (E. Maturi, personal communication) to produce the 6-km horizontal resolution grids. Because of processing and bandwidth delays, the hourly data are available with a 1.5-h lag. Comparisons between the individual buoy and GOES SSTs within the FL-ARPS domain for May 2004 are quite good, with differences in their means ranging from 0.01° to 0.37°C.

b. MODIS

MODIS SSTs are available up to 4 times per day depending on the satellite pass coverage within the FL-ARPS domain (during the following time intervals: 0300–0400, 0700–0800, 1500–1600, and 1800–1900 UTC) from a combination of both the *Aqua* and *Terra* platforms and are of high spatial resolution (1 km). The SST algorithm is based on IR retrieval methodology, yields a bulk SST estimate, and uses both mid- and far bands that are corrected for atmospheric absorption and cloud screened (Brown and Minnett 1999). The "official" algorithm was developed by the MODIS Science Data Support/Ocean Science Teams. The data used for this study were obtained from the Goddard Space Flight Center Distributed Active Archive Center (DAAC). A relatively limited study comparing MODIS SSTs and collocated skin SST measurements from the Marine-Atmospheric Emitted Radiance Interferometer indicates SST bias errors of 0.2 K and an rmse of 0.26 K (Minnett et al. 2001). MODIS versus individual buoy SST comparisons for the May 2004 FL-ARPS domain indicate nighttime differences ranging from 0.05° to 0.5°C, while daytime differences were larger, ranging from 0.2° to 0.7°C. MODIS SSTs were warmer at all buoy locations at night and cooler at all buoy locations except for 42013 during the day.

c. RTG-SST analysis

The current operational 0.5° × 0.5° RTG-SST product uses in situ (ship and buoy) and satellite-derived SST data (*NOAA-16* SEATEMP retrievals) from the Naval Oceanographic Office Major Shared Resource Center (for more details regarding the analysis see Thiébaux et al. 2003). The RTG-SSTs are used solely as a benchmark to evaluate the performance of the high-resolution SST analysis work presented here.

d. Buoy

Moored buoy data are obtained from seven sites for May 2004 (within the FL-ARPS/ADAS domain; Fig. 1) via the National Data Buoy Center (NDBC) online archive (see http://www.ndbc.noaa.gov/). Coastal-Marine Automated Network (C-MAN) stations that are located on piers, lighthouses, and beaches are not used here. The buoys use conventional thermometers to measure SST at depths ranging from 1 to 2 m. Because buoys measure the temperature at a specified depth under the surface, on the order of a meter, they are often referred to as "bulk" temperatures (rather than skin temperatures). Although satellites measure radiances that represent the temperature of a surface layer less than a millimeter thick (after the removal of atmospheric effects; Reynolds 1988), SST retrieval methodologies generally regress radiances against buoy data and as such represent bulk upper-ocean temperatures.

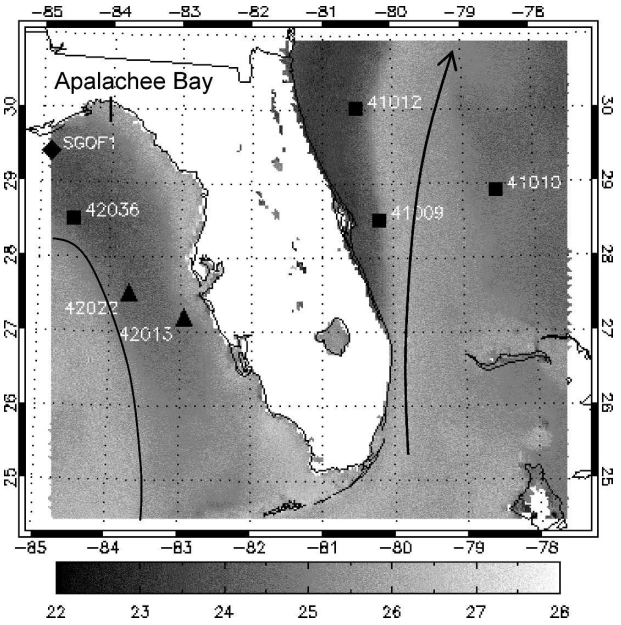

FIG. 1. Mean SSTs (shaded, °C) for May 2004 and buoy locations used for bias correction and analysis validation: NOAA buoys (squares), USF COMPS (triangles), and a C-MAN station (diamond). Approximate eastern edge of the LC is depicted by the solid line and the FC by the solid arrow.

The five NDBC buoys (41009, 41010, 41012, 42036, and SG0F1) have an SST error specification of ±1°C with 0.1°C resolution. The other two buoys used in the study are part of the University of South Florida Coastal Ocean Monitoring and Prediction System (USF COMPS) network in the Gulf of Mexico. COMPS metadata indicate that the SST accuracy for these stations is 0.005°C (see online at http://comps.marine.usf.edu/metadata/). The buoy data, which are available hourly with a 30-min latency, are used here to both 1) bias correct the satellite observations and 2) evaluate the analyses.

3. Data processing

Quality assurance (QA) is a critical component of an analysis system and should be applied to both the observations and first-guess (background) field. In particular, it is generally assumed that the background field is a good approximation of the truth—an assumption that implies, a priori, that the analysis increments are small. As an integral component of the QA process, bias estimation should take prevalence over covariance modeling (e.g., Dee and da Silva 1999) in particular to avoid spurious error variance estimates. Various QA aspects pertaining to the MODIS- and GOES-retrieved SSTs, including both bias estimation and correction as well as the removal of spurious (i.e., erroneous) SSTs,

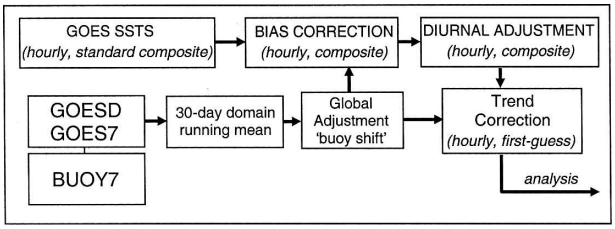

FIG. 2. Flowchart depicting the preanalysis processing of the GOES, MODIS, and buoy SSTs: Domain-averaged (zero-latency) GOES SSTs (GOESD), GOES SSTs averaged at the seven buoy locations (GOES7), and domain-averaged buoy SSTs (BUOY7).

are examined here. Herein we distinguish between the "zero latency" GOES imager product, which contains missing data, and the composite products that contain no missing data but have data of varying latency. A flowchart depicting the sequence of bias correction steps is shown in Fig. 2. The process can be summarized in the following three steps: 1) zero-latency GOES SSTs are bias corrected using the in situ buoy data. The domain-averaged buoy SSTs are first adjusted for spatial representativeness using the difference between the 30-day domain-averaged (zero latency) GOES SSTs (GOESD) and GOES SSTs averaged at the seven buoy locations (GOES7); 2) an empirical diurnal correction model is applied to mitigate the latency; and 3) a final bias correction referred to as a "trend correction" is then applied to remove any residual latency not removed by the diurnal correction. Analyses are generated using the composite product from step three above as the first guess. Aspects of each of these steps are discussed in more detail in the following sections.

a. Spurious SSTs

1) GOES

Comparisons of GOES and MODIS composites (Haines et al. 2006) for May 2004 indicated the presence (in the NESDIS processed *GOES-12* data) of glint-contaminated SSTs in the shallow shelf regions of the analysis domain, well inside the glint window (not shown). These residual glint-contaminated SSTs were removed, resulting in a maximum data loss due to glint within the FL-ARPS domain of around 40%–45% between the hours of 1600 and 1900 UTC. After removing the remaining glint data, the May 2004 innovations (i.e., MODIS minus GOES SST) were stratified by the bottom topography (Fig. 3). Nighttime MODIS SSTs are warmer than GOES with innovations that are on the order of 0.5°C and independent of depth. In contrast, daytime innovations are distinctly bimodal in the shallow regions around 25-m depth and show two separate but distinct clusters—one centered near −0.5°C (at

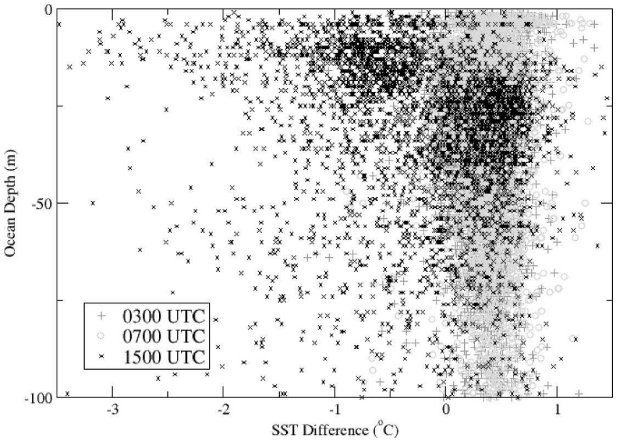

FIG. 3. MODIS minus *GOES-12* SSTs (°C) for May 2004 as a function of ocean depth (m) for daytime (1500 UTC, black x) and nighttime (0300 UTC, gray circle; 0700 UTC, plus sign) for depths ranging from 0 to 100 m.

15 m) and another centered near +0.5°C (at 30 m). The locations of these anomalous GOES SSTs lie within approximately 25 km of the coastline (not shown) and appear to be a result of bottom reflectance. As a result, daytime SSTs (1100–2300 UTC) were eliminated in *all* regions where the water depth is less than 25 m deep. For the period under consideration, this appears to be sufficient in removing the coastal warm bias.

2) MODIS

Direct broadcast MODIS SST data from the Space Science and Engineering Center (SSEC) were not available during the test period; therefore, the training data used herein were obtained from the Goddard DAAC. As a result, the SSTs were retrieved using the official MODIS Science Team SST algorithms (Brown and Minnett 1999) rather than the SSEC operational algorithm. Both data streams contain the same cloud screening flags and are, in general, quite similar. For May 2004, SSTs are cloud screened using the MODIS collection-4 algorithm, which uses approximately 14 (out of 36) spectral bands to estimate whether a given field of view is clear of clouds and/or optically thick aerosols and whether "clear" scenes are affected by cloud shadows (Ackerman et al. 1998). A multispectral approach is used to detect the presence of thin cirrus clouds and low-level stratus or nocturnal small cumulus, each of which can be difficult to detect (Ackerman et al. 1998). The identification of clouds is a somewhat subjective process in that it is based on differences between measured radiances and empirical thresholds. The threshold approach associates a certain confidence level with respect to whether or not the sky is clear. The MODIS collection-5 algorithm is now operational and available in real time from the DAAC.

The May 2004 *Terra* SSTs exhibited a relatively significant cool bias around 1600 UTC with MODIS at the 7 available buoy locations (MODIS7) on the order of 1°C cooler than the buoy SSTs (not shown). It is not clear what the source(s) of these spurious SSTs is (are); however, these data have been removed from the analyses presented here, thereby reducing the number of analyses to 3 per day for May 2004.

b. Initial bias correction

Discrepancies in regional, seasonal, and diurnal cycles between satellite and in situ SSTs are well known and underscore the need for regional bias adjustments (e.g., Kawai and Kawamura 1997). GOES sensor calibration and near-surface SST gradients can also impact measurement accuracy with hourly systematic bias variations of the bulk SST exceeding 0.6 K (Wick et al. 2002). Furthermore, in situ SSTs are generally more valuable as a mechanism to correct satellite bias rather than direct assimilation (Reynolds et al. 2005). Direct comparison with in situ buoy data can be problematic, however, as the satellite footprint is larger than a buoy point measurement. Additionally, a lack of buoy observations can make bias correction difficult. Here, we assume the buoy SSTs are unbiased, following an adjustment for spatial representativeness. There are two relatively distinct issues regarding composite bias including 1) regional and/or seasonal differences between the zero-latency GOES and buoy SSTs and 2) seasonal SST trends that result in composite warming or cooling because of latency. The latter of the two aforementioned issues are addressed here.

The monthly mean buoy time series within the analysis domain are used to bias correct both the GOES and MODIS observations. Buoy data are otherwise not used in the analyses. The buoy adjustment is made by first comparing the May 2004 GOESD SST time series (filled diamonds connected by a solid line, Fig. 4) with the GOES7 SST time series (gray shaded diamonds with dashed line in Fig. 4). The diurnal trends and amplitudes are quite similar except that the GOES7 is systematically cooler than GOESD. These differences are consistent with the locations of the buoy observed SSTs within the analysis domain, each of which, with the exception of buoy 41010, is in what tends to be the relatively cooler shallow shelf regions (e.g., see Fig. 1). The mean hourly difference between the diurnal time series of GOES7 and GOESD is used to adjust the average buoy time series for the seven locations (BUOY7) to a representative domain average (open circles, Fig. 4). The adjustment assumes that the diurnal

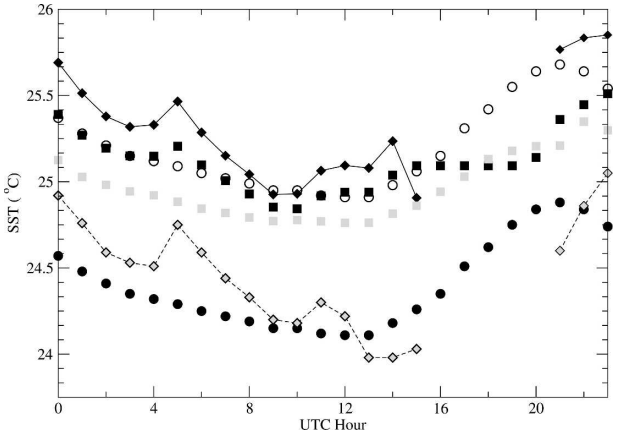

FIG. 4. Domain-averaged SST (°C) time series for buoys (filled circles), adjusted buoys (open circles), GOES SSTs averaged at the seven buoy locations (GOES7; gray filled diamonds), domain-averaged (zero latency) GOES SSTs (GOESD; black filled diamonds), GOES standard composite (black filled squares), and GOES diurnally adjusted/bias-corrected composite (gray filled squares) for May 2004.

variation of the GOES SSTs at the buoy locations is representative of the whole domain. The difference between the adjusted buoy time series and the zero-latency GOES is then used to make hourly adjustments to the zero-latency GOES SSTs. The adjustments range from −0.35°C at 0500 UTC to 0.05°C at 0900 UTC. The bias-corrected GOES SSTs are then composited in preparation for a latency adjustment. Compositing is performed hourly with new SST data replacing old data. The initial composite for this study, valid at 0000 UTC 1 May 2004, was generated using GOES SSTs from the prior week. Old data are not replaced or relaxed toward climatology but rather undergo a series of additional corrections discussed in the following two sections. In the absence of zero-latency data, such as within the glint window, the bias-corrected composite reflects the most recent hourly adjustment. As a result, during the glint window, the diurnal time series appears relatively flat (filled squares, Fig. 4). The bias correction removes the midnight SST spike at 0500 UTC, which appears to be an artifact of a midnight blackbody calibration correction implemented in response to solar heating of the instrument (Johnson and Weinreb 1996). *Terra* and *Aqua* SSTs are also bias corrected, using differences between the adjusted buoy and domain-averaged MODIS SSTs, in a separate step that precedes the analysis [MODIS bias correction (MBC); Table 1].

c. Diurnal adjustment

In addition to clouds, sun glint is problematic and is responsible for a significant loss of GOES data across the analysis domain during the 1600–2000 UTC window. For May 2004, the average latency varies across the FL-ARPS domain, ranging from a minimum of 2 h over portions of the northeast GOM and north of the Bahamas to values around 12–24 h over portions of the FC and south of the Florida Keys. Because it is desirable to preserve the true SST gradients in the composites while simultaneously avoiding the introduction of spurious SST differences, GOES composite SST gradients as a function of gridpoint separation are examined for May 2004. Two zero-latency products are shown in Fig. 5—one in which all zero-latency hourly data are used (open squares with solid line) and a second subset that uses only those zero-latency hourly composites that are deemed sufficiently clear. The top 10% of the zero-latency composites, by data volume, are considered to be clear (filled squares with solid line). The latter of the two products, considered to be the best representation of the true SST gradient, is used here to gauge the impact of latency. Also shown is an "all latency" product, referred to herein as the standard composite, which is a composite consisting of all data regardless of the latency (filled squares with dashed line, Fig. 5). This product essentially represents the worst-case scenario of the gradient error due to latency.

TABLE 1. GOES composite TC (°C) and MBC (°C) at analysis times only. Corrections are averaged over temporal windows corresponding to the times that *Terra*/*Aqua* traverse the analysis domain. Positive (negative) values indicate warming (cooling).

Time (UTC)	TC (°C)	MBC (°C)
0200–0400	0.23	−0.37
0600–0800	0.23	−0.44
1700–1900	0.31	0.03

Ideally, data latency problems would best be mitigated by a coupled ocean–atmosphere modeling system. Here, we take a more operationally feasible approach by applying a simple diurnal correction to latent data within the bias-corrected composites. An empirical methodology developed by Gentemann et al. (2003) is applied here. The Gentemann approach takes into account the diurnal variations in SST due to insolation and wind speed, both parameterization inputs. The SST adjustment (ΔSST) is described by the following empirical formula:

$$\Delta\mathrm{SST}(t, Q, u) = 0.344 \times f(t) \times [(Q - Q_o^p) - 1.444 \times 10^{-3} \times (Q - Q_o^p)^2] \times e^{-0.29u}, \quad (1)$$

where Q is the insolation, Q_o^p is a threshold insolation (set to 24 W m^{-2}), t is time, u is wind speed, and $f(t)$ is a time-dependent Fourier expansion. The Gentemann

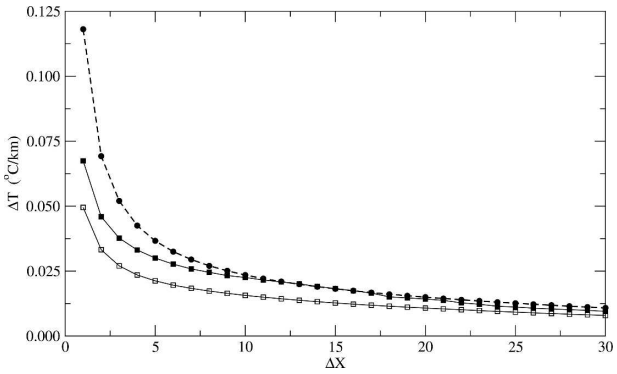

FIG. 5. May 2004 *GOES-12* domain-averaged SST gradients ΔT (°C km^{-1}) as a function of distance Δx (×6 km) between grid points, obtained from various composites including zero-latency SSTs for all hours (filled squares with solid line), zero latency using clear-sky data only (open squares with solid line), and all latency (filled circles with dashed line).

approach is a bulk parameterization with the intended inputs being the daily average near-surface wind speed and solar insolation, with Fourier coefficients derived via a nonlinear regression of collocated SSTs, insolation, and wind speeds over a 13-yr period. For May 2004, we use a combination of Mesoscale Eta Model (Black 1994) 10-m winds and GOES-derived surface insolation (Otkin et al. 2005) as inputs to the Gentemann parameterization. GOES SSTs are not available during the 1500–1900 UTC window because of glint, and thus the composite diurnal signal is significantly damped (e.g., filled black squares in Fig. 4). Tests of the Gentemann approach with the May 2004 SST composites produced afternoon SST adjustments in the GOES composites that were too small. The Gentemann approach was derived using data at the global and annual spatial and temporal scales and thus may not be representative of regions that exhibit strong diurnal and seasonal variability (Gentemann et al. 2003). For May 2004, we subtract 6 instead of 4 h from UTC in an effort to extend the diurnal warming into the late afternoon/early evening hours (e.g., Zeng and Beljaars 2005). This adjustment had the desired effect, in part, resulting in an increase in the late afternoon/early evening diurnal signal as shown in Fig. 4. No adjustments were made to the amplitude of the diurnal signal. Ultimately, an algorithm tuned to seasonal and regional variability would likely provide a better representation of the diurnal signal. The impact of the Gentemann algorithm for other months is currently being investigated.

d. Trend correction

If the diurnal adjustment were completely effective, the resulting composites should exhibit little in the way of SST differences from the adjusted buoy data. However, the bias corrected/diurnally adjusted composite time series remains on the order of 0.25°–0.5°C cooler than the adjusted buoy SSTs. Because the zero-latency GOES SSTs are actually warmer than the adjusted buoy SSTs for all hours except 0900–1000 UTC (Fig. 4), the relatively cool composite diurnal cycle must be an artifact of the time of year, as SSTs are warming and thus old SSTs will generally result in a cooling of the composites. A final adjustment, referred to as a trend correction here, applied directly to the composites is performed in which the diurnally adjusted GOES composite SSTs are shifted by an amount equal to the difference between the adjusted buoy and bias/diurnally corrected SST composite time series.

4. Analysis methodology

Analyses are performed using an optimum interpolation–type assimilation scheme originally described by Bratseth (1986) and more recently by Kalnay (2003). The Kalnay approach iterates an observation correction vector,

$$\mathbf{d}_\upsilon = [\mathbf{I} - (\mathbf{HBH}^{\mathrm{T}} + \mathbf{R})\mathbf{M}^{-1}]\mathbf{d}_{\upsilon-1} + \mathbf{d}_0, \qquad (2)$$

where $\mathbf{d}_\upsilon$ is the υth iteration of the innovation vector $\mathbf{d}_0$, $\mathbf{B}$ and $\mathbf{R}$ are the background and observation error covariance matrices, respectively, $\mathbf{H}$ and $\mathbf{H}^{\mathrm{T}}$ are transformation operators that map model variables to observation space and vice versa, the superscript T denotes transpose, $\mathbf{I}$ is the identity matrix, and $\mathbf{M}$ is a diagonal matrix. The elements of $\mathbf{M}$ are chosen to enhance the convergence of the geometric series [i.e., the term in the brackets in Eq. (2)],

$$m_{ii} = \sum_{k=1}^{N} |b_{ik} + r_{ik}|, \qquad (3)$$

where b_{ik} and r_{ik} are the elements of the $\mathbf{HBH}^{\mathrm{T}}$ and $\mathbf{R}$ matrices, respectively. Upon sufficient iteration of the correction vector [Eq. (2)], a single-pass gridpoint analysis is performed,

$$\mathbf{X}^a = \mathbf{X}^b + \mathbf{BH}^{\mathrm{T}}\mathbf{M}^{-1}\mathbf{d}_\upsilon, \qquad (4)$$

where $\mathbf{X}^a$ and $\mathbf{X}^b$ are the analysis and background vectors, respectively. Three iterations [of Eq. (2)] for the analyses presented here were performed. The background or first-guess vector used here is the GOES composite product following the trend correction (see Fig. 2). The innovation vector represents the difference between the background and observations at the observation locations. Here, the observations are composed of the MODIS SSTs. The second term on the rhs of

Eq. (4) is often referred to as the analysis increment and is a "weighted" correction to the background field. The size of the analysis increments or correction depends, in part, on the error characteristics of both the observations and background, as discussed in the following section. Three analyses per day, corresponding to the MODIS overpass times, are generated using a horizontal grid resolution of 4 km.

5. Error characteristics

The background error covariance [b_{ik}; Eq. (3)] is typically assumed to be an isotropic Gaussian function that depends on the observation-to-grid point distance and an error decorrelation length scale. The length scale is generally not constant or isotropic, however (e.g., Thiébaux 1976; Thiébaux et al. 2003; Bormann et al. 2003), and depends on a number of factors including features of interest, data density and distribution, and analysis resolution. The various methods by which these analysis parameters are estimated can be found in the literature (e.g., Gandin 1963; Thiébaux et al. 1986; Hollingsworth and Lönnberg 1986). The approach taken here, and discussed in the following section, is to apply methods by which the error decorrelation and variance are allowed to vary spatially.

a. Length scale

A feature-driven approach, in which climatological SST gradients are calculated from a monthly average of the quality-controlled hourly zero-latency GOES SSTs (Fig. 1), is applied here. The climatological SST gradients are then linearly mapped to a representative length scale via

$$L = \left(\frac{|\nabla T|_{\max} - |\nabla T|}{|\nabla T|_{\max}}\right)(L_{\max} - L_{\min}) + L_{\min}, \quad (5)$$

where $L_{\max}$ ($L_{\min}$) are the maximum (minimum) length scales (100 and 25 km, respectively), and $|\nabla T|$ ($|\nabla T|_{\max}$) is the (maximum) climatological SST gradient in the analysis domain. The lower bound, determined by trial and error, was selected so as to draw for as much analysis detail as possible without generating noisy analyses. The upper bound was chosen so as to mitigate the impact of data on one side of the Florida peninsula influencing the analysis on the other. A 9 point smoothing is applied (20 iterations) to avoid abrupt changes in length scales. A comparison of Fig. 1 and Fig. 6 indicates that the shortest length scales (dark shading) correspond to the relatively large climatological SST gradients along the western edge of the FC, the eastern edge of the Loop Current (LC), and the warm shelf water along the Florida west coast. Small length scales are also found in the shallow shelf waters of the Bahamas. Longer length scales are found in the northeast portion of the domain, where the climatological SST gradients are small. The gradient-based approach is computationally efficient and thus an attractive choice for operational applications (e.g., Thiébaux et al. 2003).

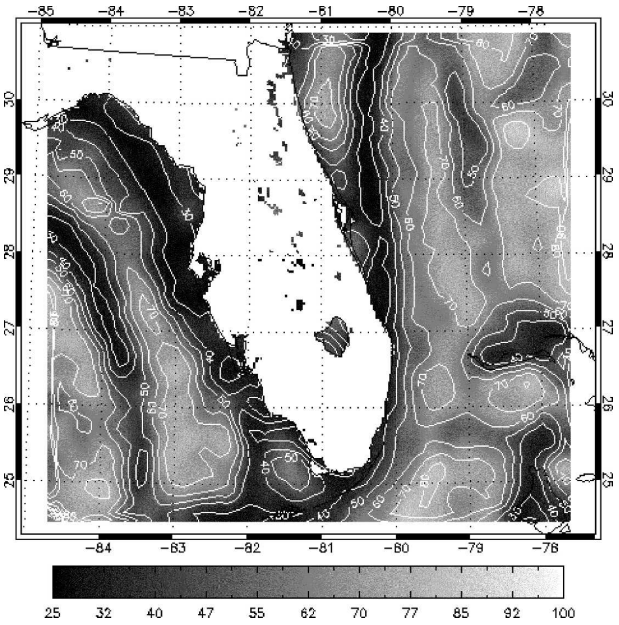

FIG. 6. Error decorrelation length scale (km) estimate obtained using Eq. (5) in text and the May 2004 SST climatology shown in Fig. 1.

b. Error variance

The background error variance is estimated from the final composite product, using the average of the squared innovations within 40 km of a given analysis grid point for May 2004. The distance was chosen to allow a sufficient number of innovations within the subregion, while at the same time keeping the number of calculations at a reasonable level. Tests whereby the error variance was calculated using larger radii showed little sensitivity. Ideally, estimates of the error variance should be tied directly to the length scale. Here, systematic bias in the data is *assumed* to be accounted for (i.e., removed) and thus any remaining variance is solely an artifact of random errors in the background field. The observation error variance is set to a constant value, 0.1°C. In reality, the average variance of the innovations contains errors from both the GOES and MODIS SSTs. An additional QC step, a background comparison test that rejects observations that differ from the background field by more than 2°C, is applied

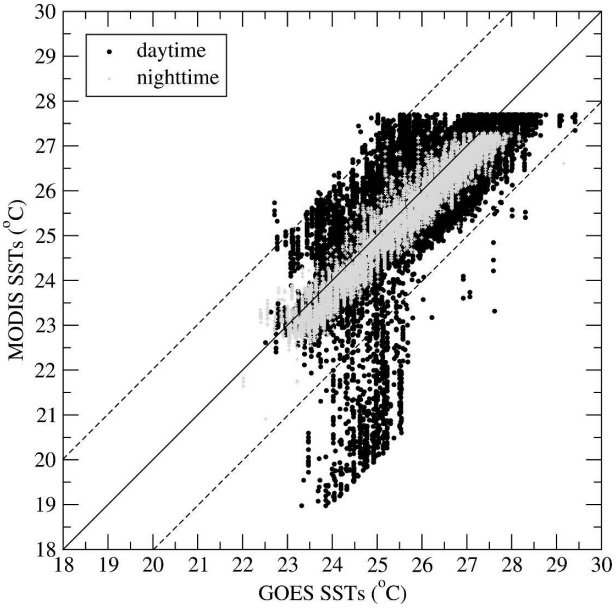

FIG. 7. GOES composite SSTs (bias corrected, diurnally adjusted, and trend corrected) versus MODIS SSTs (°C) for May 2004 centered on an approximate 1° latitude–longitude region near 27.637°N, −82.804°W. Daytime (nighttime) SSTs are delineated by the black circles (gray plus signs). Dashed lines depict ±2°C background check threshold in which MODIS SSTs are rejected (see text for additional details). Cool MODIS SSTs outside of threshold are an artifact of clouds.

prior to the calculation of the error variance. The impact of this QC application is illustrated in Fig. 7, which is a scatterplot of GOES versus MODIS SSTs over an approximately 1° latitude–longitude subregion west of Tampa, Florida, for May 2004. Nighttime SSTs are tightly clustered while daytime SSTs exhibit considerable variability—with significant outliers where the MODIS SSTs are more than 2°C cooler than the GOES composites. These outliers are a combination of thin stratiform cloud edges and jet contrails, which are not properly identified in the MODIS/DAAC SSTs, despite using only those SST data with the most stringent cloud-clearing flag.

Because of the relatively high resolution of the analysis domain (4 km), the variance calculations are performed at every other grid point. A single-pass Barnes analysis (Barnes 1964) is used to spread the variance information to the remaining grid points. Error variance statistics are calculated separately for day and night and are shown in Figs. 8a,b. The most striking features are that the nocturnal error variance estimates are 1) relatively homogeneous and 2) significantly smaller than their daytime counterpart. The largest error variances, ranging from 0.75° to 1.0°C, are confined to the northeast portion of the domain and near the

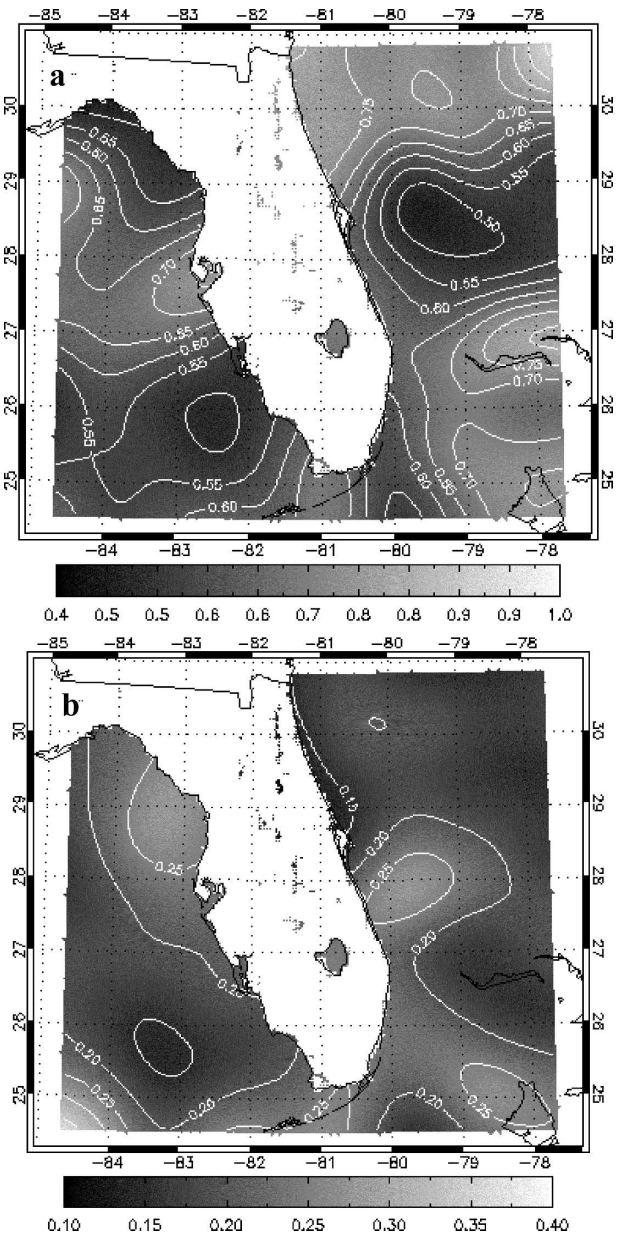

FIG. 8. Error covariance (°C^2) estimate for May 2004 during (a) day and (b) night.

Bahama Islands. In particular, the BC MODIS SSTs in the northeast corner are approximately 0.4°C warmer than the corrected GOES composites, resulting in locally higher daytime error variance estimates and possible localized biases in this region.

6. Results

Composite and analysis rmse statistics, calculated using buoy data as a surrogate for the truth, are stratified

TABLE 2. May 2004 SST rmse (°C) at the given buoy locations (day/night) for the NCEP RTG product and various stages of the composites: standard (GOES SSTs without QC or adjustments), BC, DA, and TC. Statistics correspond to analysis times only.

		Daytime composites			
Buoy	RTG	Standard	QC, BC	QC, DA	QC, BC, DA, TC
41009	0.56	0.94	1.05	0.67	0.61
41010	0.56	1.03	1.18	0.67	0.60
41012	0.56	1.21	1.34	0.88	0.75
42022	0.33	0.96	1.18	0.64	0.58
42036	0.48	0.91	1.10	0.68	0.61
		Nighttime composites			
Buoy	RTG	Standard	QC, BC	QC, DA	QC, BC, DA, TC
41009	0.83	0.61	0.62	0.61	0.61
41010	0.43	0.58	0.70	0.59	0.56
41012	0.64	0.43	0.50	0.42	0.40
42022	0.27	0.36	0.46	0.38	0.35
42036	0.58	0.33	0.31	0.33	0.36

by day/night for May 2004. The bulk statistics shown in the tables presented herein reflect a total of 40 daytime and 80 nighttime composites/analyses for May 2004. Although data from seven buoys were used to bias correct the GOES and MODIS SSTs, only five are used here for statistical comparison, as two of the buoys lack sufficient data for a point evaluation. Composite rmse is calculated for four different GOES composite products including the standard with no QC, bias corrected with QC, diurnally adjusted with QC, and the "final" product, which includes all the adjustments as discussed in section 3. The final composite product serves as the background field for the analyses presented in sections 6b and c. The rmse is estimated for analyses generated from the composite products—two different cloud masks including the confident clear and probably clear flags, anisotropic weights, and "thinned" MODIS observations.

a. Composite evaluation

The rmses for the standard composite, the intermediate composites created with the BC or DA steps only, and the final composite with all the corrections are shown in Table 2. The impact of the suite of corrections is positive during the daytime at each of the buoy locations with reductions in the rmse, from the standard composite, ranging from 0.3° to 0.5°C. The nature of the corrections is illustrated in Fig. 9. Specifically,

- the BC step cools the zero-latency GOES SSTs and thus cools the composites, thereby increasing the rmse;
- the DA improves the daytime rmse on the order of 0.3°C as the daytime composites, populated by cooler nocturnal SSTs, are warmed by the solar correction component;
- the TC warms the composites, which further reduces the rmse;

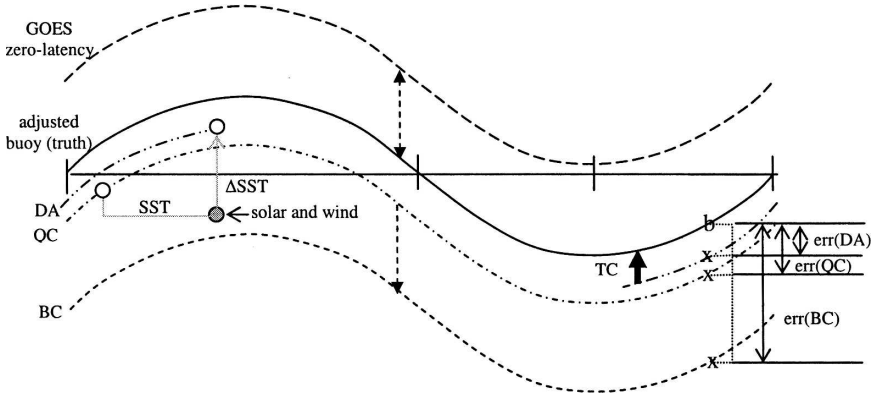

FIG. 9. Idealized sinusoidal diurnal SST time series representing various composite means: QC (dot–dashed), BC (short dashed), DA (dot–dot–dashed), and GOES zero latency (long dashed). Also shown is the adjusted buoy time series (solid). The bias correction magnitude (adjusted buoy minus GOES zero latency) is depicted by the dashed line arrows, and the TC magnitude is represented by the thick arrow. A hypothetical error estimate (err) using the buoy (labeled b) minus composite (labeled x) SST is illustrated by the thin black arrows. For simplicity, the buoy observation is assumed to lie exactly on the average diurnal time series. Also shown is an example of a daytime diurnal adjustment whereby the most recent SST is adjusted to remove the diurnal signal, propagated forward in time, and then used in tandem with the current solar radiation and 10-m wind to update a latent SST (gray arrows; see text for details).

TABLE 3. Nighttime GOES availability (total number of valid observations divided by the total possible) for May 2004.

Buoy	Availability (%)
41009	62.5
41010	34.9
41012	61.0
42022	52.2
42036	75.4

- the "best" (i.e., lowest rmse) daytime composites are those created with all but the BC adjustment, indicating that at most buoy locations, the domain-averaged zero-latency GOES SSTs are not representative of the local bias; and
- the rmses of the best daytime composites are somewhat larger (0.2°C or less) than that of the RTG, the latter of which uses (24-h average) buoy SSTs in the analyses. The time of the comparison is somewhat fortuitous for the RTG, as the daytime composite and RTG statistics presented in Table 2 correspond to the 1700–1900 UTC window only (*Aqua* overpass times), where the domain mean buoy SST is close to that of the diurnal average.

The standard GOES SST composite rmse is on the order of 0.5°C lower at night compared with both the standard and adjusted daytime composites and is also better than the RTG-SST at 4 of the 6 buoy locations. Overall, the adjustments appear to have little impact at night—an indication of the enhanced quality of the nocturnal GOES SSTs. Highlights include the following:

- The largest rmse increase associated with the BC coincides with buoy locations that have relatively large composite latencies, such as buoys 41010 and 42022 with 35% and 52% of data present, respectively (Table 3). Conversely, there is little change in the composite rmse due to the BC for locations with low latency, such as at buoy 42036.
- Nighttime winds are generally weak at the buoy locations (for May 2004) and thus the DA impact is small.
- At latent locations, the trend correction warms the May 2004 composites and thus acts to adjust the cool composites toward the buoy SSTs (e.g., Fig. 9), thereby decreasing the rmse (Table 2).

b. Isotropic analyses

Isotropic analyses were performed using all the data, a constant length scale ($L = 100$ km) and observation-to-background error variance ratio ($\sigma^2 = 0.1$), and the final GOES composite background field with all adjustments.

TABLE 4. May 2004 analysis rmse (°C) for day and night. Analyses are performed with a constant length scale ($L = 100$ km) and error variance ratio ($\sigma^2 = 0.1°C^2$) using a background field with all adjustments. Experiments are FULL (all data), THIN (subsampled with super observation data), NOMB (no MODIS bias correction), less strict cloud mask (LSCM), and variable length scale and background error covariance (VLBE).

	Isotropic, day				Anisotropic, day	
Buoy	FULL	THIN	NOMB	LSCM	THIN	VLBE
41009	0.66	0.65	0.65	0.68	0.65	0.62
41010	0.57	0.52	0.52	0.62	0.51	0.53
41012	0.72	0.65	0.66	0.75	0.63	0.68
42022	0.53	0.54	0.55	0.58	0.53	0.60
42036	0.51	0.51	0.52	0.51	0.49	0.44
	Isotropic, night				Anisotropic, night	
Buoy	FULL	THIN	NOMB	LSCM	THIN	VLBE
41009	0.64	0.63	0.66	0.61	0.62	0.63
41010	0.57	0.54	0.45	0.57	0.54	0.52
41012	0.49	0.40	0.45	0.44	0.40	0.39
42022	0.46	0.46	0.34	0.49	0.47	0.45
42036	0.33	0.33	0.42	0.32	0.33	0.30

1) COMPOSITE IMPACT

A comparison of the daytime rmse for the standard composites (second column, Table 2) and isotropic analyses using all observations (FULL; Table 4) indicate that with the exception of buoy 41009, daytime analysis rmse is lower by as much as 0.10°C, suggesting that the MODIS observations add value, albeit small, to the adjusted composites.

An examination of 5 analyses with SST differences greater than 0.25°C from that of the composite at buoy 41009 indicates the following:

- There is only one analysis (1900 UTC 24 May 2004) where the assimilation of MODIS SSTs actually reduces the rmse. For this case only, the local MODIS SST bias is consistent with the estimate given in Table 1, in which the MODIS SST is slightly cooler than the buoy SST.
- For three of the analyses, the MODIS SST is actually warmer than the buoy SST, counter to the bulk bias estimate (Table 1). Although the composite first guess is also warmer than the buoy in two of these (three) cases, the analysis increment is positive and produces analyses that are too warm.

The impact of the MODIS observations on the nighttime analyses is generally negative but small. An exception is the nighttime composite SSTs at buoy 42036, which are, in general, warmer than the buoy SSTs for May 2004. This is consistent with both the relatively low

latency at 42036 (Table 3) and the bias estimate, and produces negative analysis increments that reduce the nighttime rmse at 42036.

The rmse is also shown for analyses where the MODIS SSTs are not bias corrected (NOMB; Table 4). A comparison with the isotropic analyses (THIN; Table 4) indicates that the impact of the MODIS BC is generally small for the daytime analyses and mixed at night and that the small daytime differences are due to the small MODIS BC applied during the 1700–1900 UTC window (approximately 0.03°C; Table 1).

2) CLOUD MASK IMPACT

The MODIS SST product is accompanied by four distinct confidence levels associated with a cloud mask. Here, the impact of the two highest confidence flags (i.e., "confidently" and "probably" clear) on the analyses are summarized. The latter mask includes the confidently clear data. Comparing the two sets of analyses for May 2004 indicates that the analyses that use the confidently clear MODIS SSTs only (THIN; Table 4) yield lower rmse during the daytime and mixed results at night. The analyses that use the probably clear MODIS SSTs are, at times, better than the confidently clear during the night because of an overly conservative nocturnal cloud mask in which large amounts of "good" nighttime data are erroneously tagged with a higher probability of cloud contamination.

Recent improvements in the cloud detection algorithms have increased the percentage of nocturnal confidently clear pixels with day and night numbers that are more comparable (not shown). Despite increasing levels of sophistication in detection algorithms, cloud edges and thin cirrus remain problematic and require additional QC measures that form an integral component of any SST analysis system.

c. *Anisotropic analyses*

The anisotropic analyses were performed using thinned MODIS data [for thinning details see section 6c(2)], both constant and spatially varying length scale and error variance ratios, and the final GOES composite product with all adjustments.

1) ANISOTROPY VERSUS ISOTROPY

Although it is typical to assume that the background error covariance decorrelates isotropically in a Gaussian manner, in reality the assumption of isotropy may be invalid. In an attempt to better represent anisotropic SST features such as the FC, LC, and so forth within the analysis domain, the isotropic weights are modified by multiplying by an anisotropic component

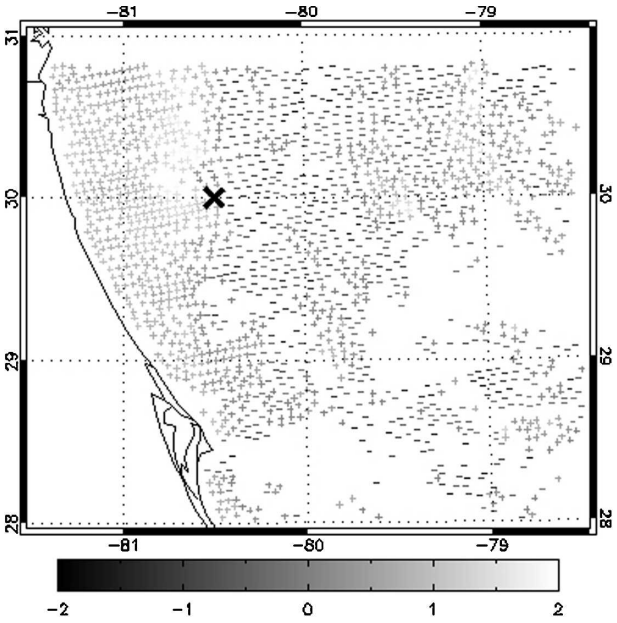

FIG. 10. Analysis innovations (MODIS minus GOES composite SST; magnitude shaded in °C) obtained from the *Aqua* MODIS SST swath and GOES composite at 1805 and 1800 UTC 9 May 2004, respectively. The black "X" depicts the location of buoy 41012.

$$\rho'_{ij} = \rho_{ij} e^{-\Delta T^2/T_s^2}, \tag{6}$$

where ρ_{ij} is the isotropic error decorrelation (Lazarus et al. 2002), ΔT is a grid point-to-observation temperature difference estimated from a 30-day climatological SST composite for May 2004 (Fig. 1), and T_s is a scale factor. Here T_s, set to 1°C, was chosen as a representative temperature difference for points separated on the order of 50 km (e.g., see Fig. 5). The climatological SST difference between two points is used to determine the degree of analysis anisotropy. As the gradient increases between the climatological SST at an analysis point and observation point, the weight decreases. For the most part, the anisotropic weight has an overall negligible impact on the analyses at the buoy locations (Table 4). In part this is an artifact of the buoy proximity to the coastline and the effective data reduction due to anisotropy, both of which tend to contribute to smaller analysis increments because of sparse data.

Given sufficient data and a *locally* anisotropic SST gradient, the analysis impact is favorable. As an example, we compare isotropic versus anisotropic analyses for an 1805 UTC 9 May 2004 MODIS overpass. The analysis innovations are displayed in Fig. 10. The relatively distinct change in the sign of the innovations occurs in association with the SST gradient along the

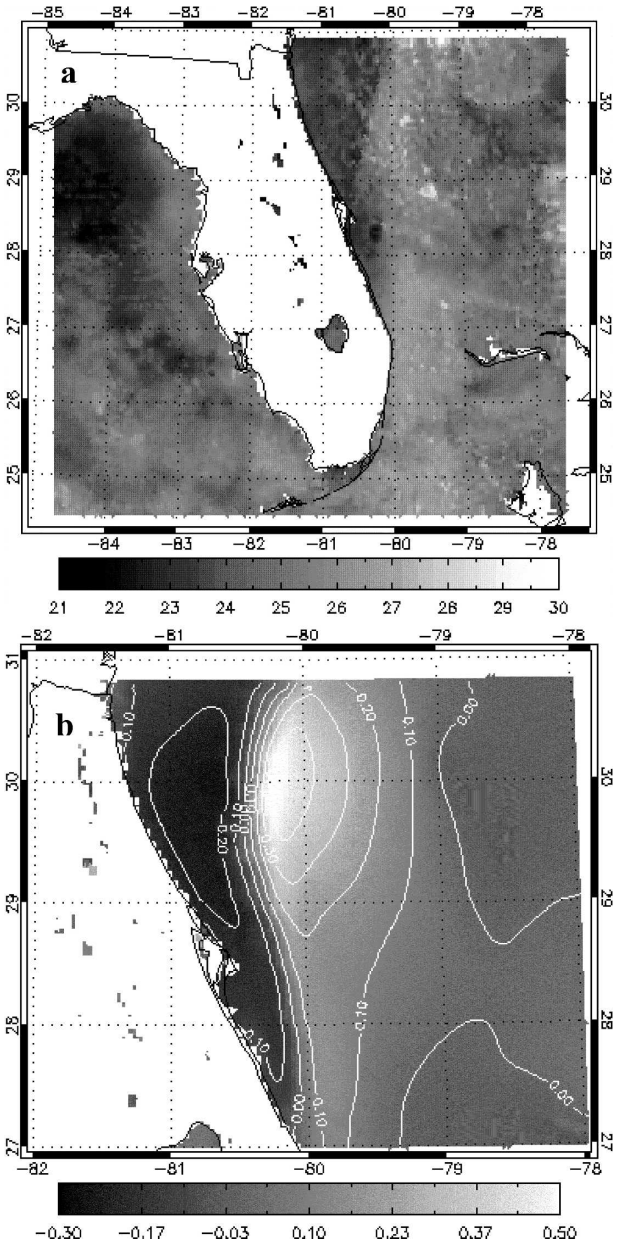

FIG. 11. The 1805 UTC 9 May 2004 (a) SST analysis (°C) and (b) local SST difference (isotropic minus anisotropic; °C).

western boundary of the FC. The positive (negative) innovations to the west (east) of the FC indicate that the MODIS observations are warmer (cooler) than the background field. The analysis and a difference plot between the isotropic and anisotropic analyses are shown in Figs. 11a,b. These figures illustrate that the isotropic analysis spreads the innovations equally in all directions, producing an analysis that appears to be too cool in the coastal waters and too warm over the western edge of the FC. Conversely, the anisotropic analysis preferentially spreads the innovations—warming the cool wedge along the coastline where there are positive innovations and cooling the western edge of the FC where there are negative innovations—thereby decreasing the SST gradient in the composite.

2) DATA THINNING IMPACT

To avoid analysis convergence problems due to dense observations (Bratseth 1986), a simple "thinning" algorithm is employed that generates super observations by averaging neighboring observations within a specified distance of one another. The thinning distance used here is set to 4 km—the resolution of the analysis grid. The analysis resolution is not the only relevant factor in determining the potential impact of the observations, as data distribution and features of interest are also important. However, because the analysis system is designed for operational use, this simple data thinning approach is economical. It would also be possible to expedite the analysis through algorithm enhancements such as parallelization. The thinning, which also acts as a simple smoother, does not generally produce evenly spaced observations, nor does it map the observations to a regular grid.

Both thinned and unthinned analysis errors are shown in Table 4. In general, differences are small, with the thinned analysis rmse smaller—an artifact of improved analysis convergence—and the reduction in the number of observations greatly reduces computation time for the analyses without degrading them. An analysis using 150 000 MODIS observations takes on the order of 30 min to run while the same thinned analysis with approximately 8000 superobservations was assimilated in under a minute.

3) SPATIALLY VARYING ERROR COVARIANCE AND LENGTH SCALE

A nighttime case with variable length scale is presented for a 0410 UTC 20 May 2004 *Terra* pass for which the analysis–buoy (42036) difference is on the order of 0.2°C (compared with 0.6°C for the fixed length scale analysis). By choosing a nighttime analysis we can better isolate the impact of the length scale because the error variance is nearly spatially homogeneous. Buoy 42036 resides in a relatively cool SST region bordered by the warmer LC and shelf waters to the west and east, respectively (see Fig. 1), and is approximately 0.8°C cooler than the composite for this particular analysis. Using thinned observations, the analysis innovations shown in Fig. 12 indicate that, in general, the GOES composite is systematically warmer

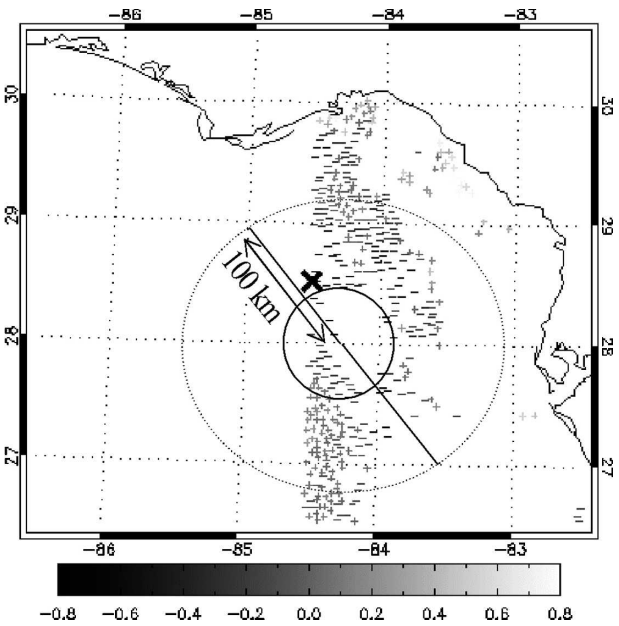

FIG. 12. As in Fig. 10 but for a *Terra* pass at 0410 UTC 20 May 2004. The black "X" denotes the location of buoy 42036. Circles represent the isotropic weighting *e*-fold distances associated with the fixed length scale (100 km) analyses and the variable length scale analyses (approximately 30 km at this point; see Fig. 6).

than the MODIS SSTs along a northwest–southeast axis. This axis runs parallel to the climatological isotherms and, more importantly, corresponds to a region of enhanced SST gradient and thus smaller length scales (Fig. 6). Also, because the variable length scale estimate at buoy 42036 is smaller than that used in the fixed length scale analysis (approximately 30 versus 100 km), the analysis increment is composed of primarily negative innovations as the impact of the positive innovations directly to the northeast and those to the southeast are reduced.

Though it is a single case, these results indicate that a judicious selection of a representative length scale can indeed be beneficial to an analysis system. To ensure that the locations of the prominent SST features within the analysis domain are accurately represented, estimates of the climatological SST gradient should probably not extend much beyond a month.

7. Discussion and conclusions

An SST analysis system designed to initialize short-term atmospheric model forecasts is presented and evaluated for a month-long period in May 2004. System inputs include retrieved SSTs from GOES and MODIS. The GOES SSTs are processed and composited via a sequence of quality control, bias correction, a diurnal correction for latency, and a final trend correction for residual latency. Prior to assimilation, the MODIS SSTs are bias corrected and checked against the GOES composite products that comprise the background field. The bias correction of both datasets is driven by an adjusted domain-averaged diurnal buoy time series. With the exception of the bias correction, buoy data are withheld from the analyses and are used instead to evaluate both the composites and analyses. Although assessment is limited as a result of the few buoy observations within the analysis domain, results indicate that the most significant analysis system improvement is a reduction in the daytime buoy/GOES composite rmse, on the order of 0.3°–0.5°C, obtained via the bias correction and adjustments for latency.

Eighty nighttime and forty daytime analyses are systematically repeated for different experimental configurations designed to test the impact of observation distribution, observation error, background error decorrelation, data reduction, and anisotropy. For May 2004, the nighttime cloud mask is too conservative, often removing good SST data and thereby degrading the analyses. Within regions of significant climatological SST gradients, cases are identified where anisotropy appears to improve the analysis, given sufficient data, though the monthly rmse scores are not universally reduced. Data thinning is shown to both reduce rmse and, more importantly, to enhance the computational efficiency of the analysis system. Nocturnal error variance estimates obtained from squared differences between the GOES composite and MODIS SSTs are roughly half that of the daytime error variance and are relatively spatially homogeneous. A spatially varying error decorrelation length scale, determined from a 30-day climatological SST gradient, is also introduced. Comparisons between the nighttime analyses with and without spatially varying length scale and error variance indicate that for regions where the innovations tend to be well correlated with distinct and persistent SST gradients (e.g., LC), the variable length scale tends to reduce the analysis rmse. Based on these findings, the following analysis configuration is recommended:

1) daytime composites—all adjustments;
2) nighttime composites—no adjustments (if significant latency, apply TC);
3) use less-restrictive cloud mask during the night (with background error check);
4) use the anisotropic weights and varying error decorrelation length scale;
5) apply spatially uniform (varying) nocturnal (daytime) error variance; and
6) thin data.

For operational purposes, estimates of the error variance, length scale, and anisotropy will be derived from a running 30-day SST climatology. Although alternative approaches exist such as a multiyear climatology, regional SST features are sufficiently dynamic (e.g., meandering of the LC, eddy shedding along the western boundary of the FC, etc.) such that longer-term climatological SSTs may not be representative of the actual gradients for a given analysis. The averaging period can be extended, if necessary, in the presence of persistent cloud cover. The SST analysis system presented here is designed to initialize real-time high-resolution short-term regional atmospheric forecasts, and as such, aspects of the work reflect our attempt to develop a computationally efficient prototype. Regardless, enhancement of the current configuration is both possible and desirable. From the composite perspective the bias correction might be improved by introducing additional data such as AVHRR, while regional/seasonal and platform tuning of the Gentemann et al. (2003) SST adjustment may act to better capture the full diurnal SST amplitude. Ultimately, regional SST coefficients for both the GOES and MODIS platforms as well as the assimilation of microwave SSTs from the Advanced Microwave Scanning Radiometer-Earth Observing System (AMSR-E) might prove more beneficial for improving regional analyses. Although the AMSR-E is capable of penetrating nonprecipitating clouds, it is of comparatively coarse resolution (on the order of 25 km) and thus it remains unclear how best to integrate these data into a high-resolution analysis. Timeliness remains an issue for all operational system inputs.

Acknowledgments. This research was supported by COMET Grant S04-44701.

REFERENCES

Ackerman, S. A., K. I. Strabala, W. P. Menzel, R. A. Frey, C. C. Moeller, and L. E. Gumley, 1998: Discriminating clear sky from clouds with MODIS. *J. Geophys. Res.,* **103** (D24), 141–157.

Barnes, S. L., 1964: A technique for maximizing details in numerical weather map analysis. *J. Appl. Meteor.,* **3,** 396–409.

Black, T. L., 1994: The new NMC mesoscale Eta model: Description and forecast examples. *Wea. Forecasting,* **9,** 265–278.

Bormann, N., S. Saarinen, G. Kelly, and J.-N. Thépaut, 2003: The spatial structure of observation errors in atmospheric motion vectors from geostationary satellite data. *Mon. Wea. Rev.,* **131,** 706–718.

Bratseth, A. M., 1986: Statistical interpolation by means of successive corrections. *Tellus,* **38A,** 439–447.

Brewster, K., 1996: Implementation of a Bratseth analysis scheme including Doppler radar data. Preprints, *15th Conf. on Weather Analysis and Forecasting,* Norfolk, VA, Amer. Meteor. Soc., 92–95.

Brown, O. B., and P. J. Minnett, 1999: MODIS infrared sea surface temperature algorithm theoretical basis document version 2.0. Rosenstiel School of Marine and Atmospheric Science, University of Miami, Internal Doc. under NASA Contract NAS5-31361, 91 pp.

Chelton, D. B., 2005: The impact of SST specification on ECMWF surface wind stress fields in the eastern tropical Pacific. *J. Climate,* **18,** 530–549.

——, and F. J. Wentz, 2005: Global microwave satellite observations of sea surface temperature for numerical weather prediction and climate research. *Bull. Amer. Meteor. Soc.,* **86,** 1097–1115.

Dee, D. P., and A. M. da Silva, 1999: Maximum-likelihood estimation of forecast and observation error covariance parameters. Part I: Methodology. *Mon. Wea. Rev.,* **127,** 1822–1834.

Donlon, C., 2002: Global Ocean Data Assimilation Experiment (GODAE) High Resolution Sea Surface Temperature Pilot Project (GHRSST-PP). Strategy and Initial Implementation Plan, GHRSST-PP Science Team, 47 pp.

Gandin, L. S., 1965: *Objective Analysis of Meteorological Fields*. Israel Program for Scientific Translations, 242 pp.

Gentemann, C. L., C. J. Donlon, A. Stuart-Menteth, and F. J. Wentz, 2003: Diurnal signals in satellite sea surface temperature measurements. *Geophys. Res. Lett.,* **30,** 1140, doi:10.1029/2002GL016291.

Glenn, S. M., and M. F. Crowley, 1997: Gulf Stream and ring feature analyses for forecast model validation. *J. Atmos. Oceanic Technol.,* **14,** 1366–1378.

Haines, S. L., G. Jedlovec, S. Lazarus, and C. Calvert, 2006: A MODIS sea surface temperature composite product. Preprints, *14th Conf. on Satellite Meteorology and Oceanography,* Atlanta, GA, Amer. Meteor. Soc., CD-ROM, P4.24.

He, R., R. W. Helber, R. H. Weisberg, H. Zhang, and F. Muller-Karger, 2004: Merging multiple satellite sea surface temperature products: A near-real-time cloud-free, sea surface temperature analysis for the southeast Atlantic coastal ocean. Preprints, *2004 Ocean Sciences Meeting,* Portland, OR, Amer. Geophys. Union.

Hollingsworth, A., and P. Lönnberg, 1986: The statistical structure of short-range forecast errors as determined from radiosonde data. Part I: The wind field. *Tellus,* **38A,** 111–136.

Johnson, R. X., and M. P. Weinreb, 1996: GOES-8 Imager midnight effects and slope correction, in GOES-8 and beyond. *Proc. Soc. Photo-Opt. Instrum. Eng.,* **2812,** 596–607.

Kalnay, E., 2003: *Atmospheric Modeling, Data Assimilation, and Predictability.* Cambridge University Press, 341 pp.

Kawai, Y., and H. Kawamura, 1997: Seasonal and diurnal variability of differences between satellite-derived and in situ sea surface temperatures in the south of the Sea of Okhotsk. *J. Oceanogr.,* **53,** 343–354.

Lazarus, S. M., J. D. Horel, and C. M. Ciliberti, 2002: Application of a near-real-time analysis system in complex terrain. *Wea. Forecasting,* **17,** 971–1000.

Lorenc, A. C., R. S. Bell, and B. Macpherson, 1991: The Meteorological Office analysis correction data assimilation scheme. *Quart. J. Roy. Meteor. Soc.,* **117,** 59–89.

Maturi, E., A. Harris, C. Merchant, X. Li, and B. Potash, 2006: Geostationary sea surface temperature products (current and future). Preprints, *14th Conf. on Satellite Meteorology and Oceanography,* Atlanta, GA, Amer. Meteor. Soc., CD-ROM, P4.22.

Minnett, P. J., R. O. Knuteson, F. A. Best, B. J. Osborne, J. A. Hanafin, and O. B. Brown, 2001: The Marine-Atmospheric Emitted Radiance Interferometer (M-AERI), a high-accuracy, sea-going infrared spectroradiometer. *J. Atmos. Oceanic Technol.,* **18,** 994–1013.

O'Neill, L. W., D. B. Chelton, S. K. Esbensen, and F. J. Wentz, 2005: High-resolution satellite measurements of the atmospheric boundary layer response to SST variations along the Agulhas Return Current. *J. Climate,* **18,** 2706–2722.

Otkin, J. A., M. C. Anderson, J. R. Mecikalski, and G. R. Diak, 2005: Validation of GOES-based insolation estimates using data from the U.S. Climate Reference Network. *J. Hydrometeor.,* **6,** 460–475.

Reynolds, R. W., 1988: A real-time global sea surface temperature analysis. *J. Climate,* **1,** 75–87.

——, and T. M. Smith, 1994: Improved global sea surface temperature analyses using optimum interpolation. *J. Climate,* **7,** 929–948.

——, H.-M. Zhang, T. M. Smith, C. L. Gentemann, and F. Wentz, 2005: Impacts of in situ and additional satellite data on the accuracy of a sea-surface temperature analysis for climate. *Int. J. Climatol.,* **25,** 857–864.

Smith, N., 2001: Report of the GODAE high resolution SST workshop, 30th October–1st November 2000. International GODAE Project Office Rep., 64 pp. [Available from International GODAE Project Office, Bureau of Meteorology, Melbourne 3001, Australia.]

Thiébaux, H. J., 1976: Anisotropic correlation functions for objective analysis. *Mon. Wea. Rev.,* **104,** 994–1002.

——, H. L. Mitchell, and D. W. Shantz, 1986: Horizontal structure of hemispheric forecast error correlations for geopotential and temperature. *Mon. Wea. Rev.,* **114,** 1048–1066.

——, E. Rogers, W. Wang, and B. Katz, 2003: A new high-resolution blended real-time global sea surface temperature analysis. *Bull. Amer. Meteor. Soc.,* **84,** 645–656.

Walker, N., S. Myint, A. Babin, and A. Haag, 2003: Advances in satellite radiometry for the surveillance of surface temperatures, ocean eddies and upwelling processes in the Gulf of Mexico using GOES-8 measurements during summer. *Geophys. Res. Lett.,* **30,** 1854, doi:10.1029/2003GL017555.

Warner, T. T., M. N. Lakhtakia, J. D. Doyle, and R. A. Pearson, 1990: Marine atmospheric boundary layer circulations forced by Gulf Stream sea surface temperature gradients. *Mon. Wea. Rev.,* **118,** 309–323.

Wick, G. A., J. J. Bates, and D. J. Scott, 2002: Satellite and skin-layer effects on the accuracy of sea surface temperature measurements from the GOES satellites. *J. Atmos. Oceanic Technol.,* **19,** 1834–1848.

Xue, M., K. K. Droegemeier, and V. Wong, 2001: The Advanced Regional Prediction System (ARPS)—A multiscale nonhydrostatic atmospheric simulation and prediction tool. Part I: Model dynamics and verification. *Meteor. Atmos. Phys.,* **75,** 161–193.

Young, G. S., and T. D. Sikora, 2003: Mesoscale stratocumulus bands caused by Gulf Stream meanders. *Mon. Wea. Rev.,* **131,** 2177–2191.

Zeng, X., and A. Beljaars, 2005: A prognostic scheme of sea surface skin temperature for modeling and data assimilation. *Geophys. Res. Lett.,* **32,** L14605, doi:10.1029/2005GL023030.